Journal of Catalysis **199,** 193–201 (2001)
doi:10.1006/jcat.2000.3141, available online at http://www.idealibrary.com on IDEAL®

Time-Resolved XANES Investigation of CuO/ZnO in the Oxidative Methanol Reforming Reaction

T. L. Reitz,* P. L. Lee,† K. F. Czaplewski,* J. C. Lang,† K. E. Popp,* and H. H. Kung*,[1]

*Department of Chemical Engineering, Northwestern University, Evanston, Illinois 60208-3120; and †Advanced Photon Source, Argonne National Laboratory, Argonne, Illinois 60439

Received July 10, 2000; revised November 13, 2000; accepted December 6, 2000; published online March 21, 2001

CuO/ZnO catalysts were examined by time-resolved X-ray absorption spectroscopy during oxidative reforming of methanol. Under low oxygen conversion conditions, Cu^{2+} was the dominant copper species and combustion of methanol to carbon dioxide and water was the primary reaction. After complete oxygen conversion, Cu^{2+} was reduced to Cu^0 while the principal activity of the catalyst shifted to steam reforming, where the dominant product was hydrogen. Cu^+ was observed as a transient species in the reduction of Cu^{2+} to Cu^0 and no activity was attributed to it. Increasing the oxygen partial pressure increased the rate of reduction of Cu^{2+}. This observation was attributed to a heating effect associated with an enhancement of the combustion rate. Additional experiments showed that the catalyst could recover its original activity after a reduction/oxidation cycle.

Key Words: **autothermal; methanol; $CuO/ZnO/Al_2O_3$; oxidative reforming; XANES.**

1. INTRODUCTION

While the elucidation of many of the surface and bulk properties of a catalyst can be obtained *ex situ*, the experimental examination of a catalyst system operating under reaction conditions remains a challenging task. However, information from such *in situ* characterization would be directly relevant to catalysis. Transient *in situ* spectroscopic characterization of catalysts, especially when coupled with isotopic labeling, has been shown to be very valuable. When the method is applied properly, information on the nature and activity of adsorbed reaction intermediates and the active solid phase can be obtained. Time-resolved near-edge X-ray absorption spectroscopy (XANES) is one such *in situ* technique which can generate information on the oxidation state of the metal cation in the active phase. XANES has been used extensively for *in situ* investigations of methanol synthesis catalysts (1–3), Ni molybdates for HDS and partial oxidation (4), and has been used to examine the V–P oxide catalysts in the partial oxidation of butane (5).

The autothermal reforming of methanol, also known as oxidative methanol reforming (OMR) has been investigated as a means to supply H_2 for automotive fuel cell systems (6–15). In this process, methanol and steam are supplied together with air to the reactor system. The ratio of the three reactants is such that the overall reaction is thermal-neutral or only modestly exothermic. Although it produces less hydrogen per mole of methanol compared with steam reforming, OMR does not require a supply of external heat. As a result, the reactor systems are significantly less complicated and more suitable for mobile applications.

The stoichiometry of the OMR reaction at an oxygen/methanol ratio of 0.25 is shown as Eq. [1].

$$\begin{gathered}CH_3OH + 1/4O_2 + 1/2H_2O = CO_2 + 5/2H_2 \\ \Delta H^{\circ}_{298^{\circ}C} = -12.0 \text{ kJ/mol.}\end{gathered} \quad [1]$$

Kumar *et al.* have shown that high reforming activity could be realized using an industrial $CuO/ZnO/Al_2O_3$ catalyst with only a minor decrease in H_2 yield compared to steam reforming (11, 12). H_2 product compositions of greater than 55% (dry), while maintaining less than 1% CO, were observed for high methanol conversions. Additionally, the exothermic nature of the reaction allowed for rapid reformer startup of less than 200 s. Rapid response to load changes, necessary for mobile applications, was also observed.

It is widely accepted that the active phase for steam reforming (Eq. [2]) over Cu–Zn oxide catalysts is metallic copper (6–10). However, for OMR it has been shown that distinctly different reactions occur in different sections of the reactor, depending on the oxygen partial pressure (14, 15).

$$\begin{gathered}CH_3OH + H_2O = CO_2 + 3H_2 \\ \Delta H^{\circ}_{298^{\circ}C} = 130.9 \text{ kJ/mol}\end{gathered} \quad [2]$$

[1] To whom correspondence should be addressed. E-mail: hkung@northwestern.edu. Fax: (847)-467-1018.

0021-9517/01 $35.00

$$CH_3OH + 3/2O_2 = CO_2 + H_2O$$
$$\Delta H_c^\circ = 726.6 \text{ kJ/mol.} \quad [3]$$

When the conversion of O_2 was low, methanol combustion (Eq. [3]) was the dominant reaction, and the copper in the catalyst remained in the oxidized state. Under these conditions H_2 selectivity was very low and the active catalytic phase was Cu^{2+}. In the region of high or complete O_2 conversion such that the partial pressure of O_2 was very low, H_2 was the dominant product observed and the steam reforming of methanol was the dominant reaction (Eq. [2]). It was postulated that in this region of the reactor, the reduced form of the copper was the active phase. However, it was not known whether any of the oxidized copper phases (Cu^+ or Cu^{2+}) contributed to this reaction or how rapid was the transition from these oxidized forms to metallic copper. In addition, a typical catalytic system for automobile applications will be subjected to hundreds of usage cycles, causing the catalyst to undergo many oxidation and reduction cycles. Consequently, a thorough investigation of this transition could yield useful information for catalyst development.

Time-resolved XANES is a technique particularly suited to address rapid oxidation state changes (<300 ms) under transient operations (16, 17). For example, in the study of butane partial oxidation over V–P–O, by correlating the transient behavior of the reaction products to the vanadium oxidation states, it was concluded that the activation of butane requires V^{5+} (5). The objective of the present work was to apply the transient XANES technique to examine the copper oxidation state of CuO/ZnO catalysts during the OMR reaction. In particular, the question of whether metallic copper is necessary for H_2 formation was addressed. Experiments were conducted with samples of different copper contents and different inlet O_2 concentrations.

2. EXPERIMENTAL

2.1. Time-Resolved XANES

In situ time-resolved XANES measurements of the copper K absorption edge were obtained using the bending-magnet beamline, 1-BM, at the Advanced Photon Source at Argonne National Laboratory. In time-resolved XANES, the X-ray beam is diffracted horizontally into a divergent beam by an elliptically bent Si (220) crystal. The crystal is positioned such that the foci of the ellipse are on the X-ray source and the sample. The incoming X-ray hits the crystal at different points along its length thereby varying the Bragg angle. Because the energy of an X-ray varies directly with the Bragg angle, the defracted X-rays will produce a spectrum of varying energies. The advantage of the bent crystal technique is that the absorbance edge of an element can be accumulated in a continuous manner because a full XANES spectrum can be recorded simultaneously.

The Si (220) curved crystal monochromator, installed at the 1BM beamline at APS, is capable of generating a few hundred to 1 keV bandwidth of X-rays in the energy range from 6.5 to 20 keV. To prevent thermal distortions and limit thermal equilibration time, the $355 \times 32 \times 0.8\,mm^3$ Si (220) crystal was cooled by an In/Ga liquid metal bath. Data were recorded in the transmission mode by a charge-coupled device (CCD) detector developed by M. Hoffberg and B. Rodnicks of the APS SRI-CAT. The CCD had a dimension of 512×556 pixels, with a pixel size of 57 μm and a potential frame rate of 50 frames/s. The CCD data were collected at a rate of 0.35 s/spectrum, and then reduced to absorbance spectra by employing an IDL-based program developed by J. C. Lang at the APS. Copper foil and wafers of commercial CuO (Aldrich, 99.99%) and Cu_2O powder (Aldrich, 99.5%) were used as calibration standards. These standards were placed next to the *in situ* cell and their spectra were recorded before and after each experiment.

2.2. Reaction System

The flow system used is shown in Fig. 1. The catalyst wafer was prepared by pressing about 10 mg of catalyst powder into a thin disk (1 cm diameter) in a die to 6 tons. A wafer ($\sim 0.5 \times 1\,cm^2$) was then cut from the disk and was placed into a stainless steel *in situ* cell (Fig. 2). Since the X-ray beam size was only 1–2 mm, only a small portion of the wafer was probed. The sample cavity of the cell was 6 mm wide by 13 mm long by 9 mm deep. The thin sample wafer was positioned in the center of the cavity supported by loosely packed quartz wool, and as close as possible to the tip of the thermocouple inserted into the thermowell. This thermocouple reading was assumed to be the sample temperature. The gaseous reaction mixture was fed into the sample cavity through the opening on one side and exited through the same opening as the thermowell.

Methanol and water were supplied by saturating N_2 and O_2 (Matheson UHP) carriers, respectively, in two sets of jacketed saturators maintained by external temperature baths. The total flow rates were kept at 100 ml/min (STP) by Brooks model 5850E mass flow controllers. The feed consisted of 30 vol% methanol, 20% H_2O, 3.5% to 12.5% O_2, and the balance N_2. Steady state oxidation and reforming activities were determined by on-line GC analysis (HP 6890) using two TCD detectors incorporating an 8 ft by 1/8 in. OD HayeSep Q column (for CH_3OH, H_2O, CO_2, and HCOOH using He as a carrier), and a 10 ft by 1/8 in. OD molecular sieve 13X column (for O_2, N_2, CO, H_2 using Ar as a carrier) for gas separation. Reactant flows were also monitored continuously with a SRS 200 residual gas analyzer (RGA).

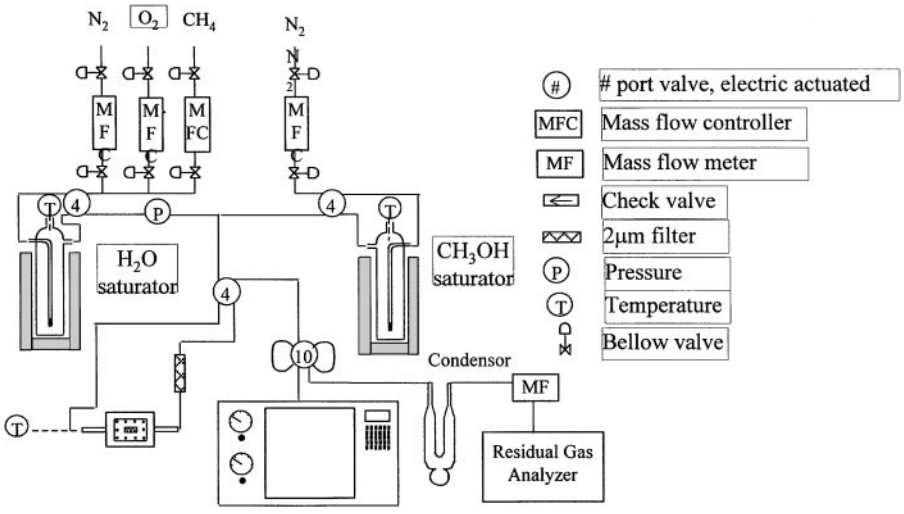

FIG. 1. Schematic drawing of the reaction system for the oxidative methanol reforming reaction.

Quantitative comparison of the transient changes in the reaction products with changes in the catalyst sample was difficult in this apparatus for the following reasons. First, because of the positioning of the thermocouple, the exact temperature of the catalyst wafer was not known, especially if there was any significant temperature gradient along the wafer. Second, there was substantial back-mixing of gas in the water trap and, to a lesser extent, in the sample chamber. Finally, the wafer occupied only a small portion of the volume in the sample chamber. Thus, there was significant bypassing of gas over the wafer.

After the catalyst wafer was placed in the sample cell, normal to the X-ray beam, and the reactant gas mixture was passed through the sample cell, the temperature was raised at a rate of 5°C/min to 180°C, measured by a thermocouple probe placed in the *in situ* cell. Steady state oxidation activity was then determined at 180°C. The temperature was then increased to 240°C at 2°C/min as XANES, RGA, temperature, and flow rate data were monitored simultaneously. At 240°C the activity was again determined by GC analysis. Afterward, the reactor was cooled at 10°C/min while XANES, RGA, temperature, and flow meter data were monitored. In some experiments, an additional cycle of heating and cooling was performed. Mass balance generally exceeded 98%. The oxygen conversions were calculated using Eq. [4],

$$\mathrm{O_2\ conversion} = \frac{3/2[\mathrm{CO_2}] - 1/2[\mathrm{H_2}]}{3/2[\mathrm{CO_2}] - 1/2[\mathrm{H_2}] + [\mathrm{O_2}]}, \qquad [4]$$

where the concentrations were determined at the reactor exit, and the coefficients were derived from the stoichiometry of the reactions. An analogous definition can be written for methanol using carbon containing species. The products detected included H_2, CO_2, CO, H_2O, CH_2O, HCOOH, and CH_3OCH_3. Product distributions are reported as molar percentages of the total product unless otherwise specified.

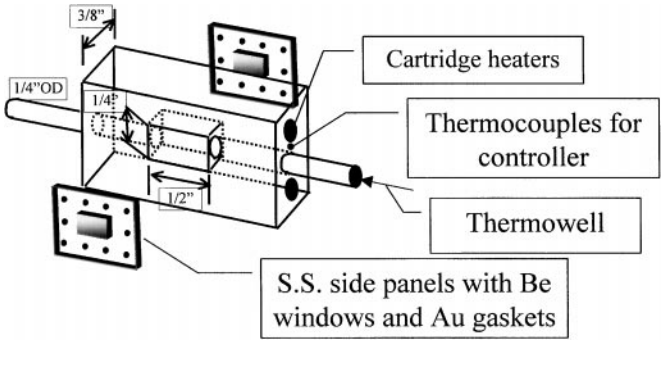

FIG. 2. Schematic drawing of the *in situ* XANES cell.

2.3. *Catalyst Characterization*

Temperature-programmed reduction (TPR) was conducted in a tubular reactor using a flow of 5% H_2/Ar (Matheson) at 60 ml/min with a temperature ramp rate of 5°C/min (19–21). The oxygen impurity in the H_2/Ar feed was scrubbed by a MnO trap regenerated periodically by H_2 treatment at 450°C. Water generated during the TPR run was removed by a molecular sieve trap. A TCD detector, with output to a computer, was used to monitor the H_2 uptake. The signal was calibrated by 1-ml pulses of UHP Ar (Matheson) at the end of the experiment. The system was calibrated by reducing CuO samples in H_2/Ar with mass balance closure of greater than $98 \pm 2\%$. All samples were untreated prior to the TPR measurements. Conditions of each run were controlled in order to obtain a high signal-to-noise ratio by adjusting the characteristic number K, Eq. [5], to approximately 400 s^{-1} according to Monti and

Baiker (22).

$$K = \frac{S_o}{VC_o}\ (s^{-1}), \qquad [5]$$

Where S_o is the quantity of reducible species in the sample (μmol), V is the volumetric flow rate (ml/s), and C_o is the initial H_2 content in the feed (μmol/ml).

2.4. Catalyst Preparation

Pure CuO was prepared by precipitation of the nitrate salt with $NaHCO_3$. After the sample was washed to remove the Na^+, the filter cake was dried at 100°C for 24 h and then calcined in air at 350°C for 6 h.

The CuO/ZnO samples were prepared by coprecipitation of the nitrate salts ($Cu(NO_3)_2$ 4.2 g @ 14 g/l, $Zn(NO_3)_2$ 13 g @ 43 g/l) by dropwise addition of Na_2CO_3 (10 g @ 33 g/l) at 80°C. The precipitate was then aged at 80°C with stirring for 60 min, filtered, and washed with warm deionized water. The filter cake was calcined at 400°C overnight. The commercial catalyst was supplied by BASF (K-110) and consisted of 40%/40%/20% by weight $CuO/ZnO/Al_2O_3$ as reported by the vendor.

2.5. Data Analysis

The XANES data were analyzed by factorial analysis (23). XAFactor, a Mathematica-based program for factorial analysis, was employed for the data analysis (24). The advantage of this technique compared with a linear combination fit is that all data can be analyzed simultaneously, giving a more complete picture of the relative change of the oxidation state. Furthermore, information about the number of factors needed to describe the system is not required before the actual experiment. Instead, standards can be fit to the data to test the likelihood that the standard is present in a given sample. If a combination of the factors can recreate the spectra of a standard within acceptable error, the standard is a likely component in the sample. In this technique, the matrix $[D]_{m\times n}$ containing data of X-ray absorption as a function of photon energy and time is decomposed into a time-dependent $[A]_{m\times i}$ matrix and a time-independent $[L]_{i\times n}$ matrix by least-squares fit (Eq. [6]):

$$[D]_{m\times n} = [A]_{m\times i}[L]_{i\times n}. \qquad [6]$$

The vectors in the [L] matrix are the factors which, when weighted by the components in the [A] matrix, compose the observed spectra. These factors are orthogonal. Theoretically, in the absence of any experimental error or noise, the number of factors needed to reproduce the observed spectra exactly equals the number of chemical species in the sample. Therefore, in these experiments, since copper can exist in oxidation states of 0, I, and II, three factors were chosen to analyze all of the data. An error estimation technique, also developed by Malinowski and Howery (23), is available to determine whether three is an appropriate number of factors for a given group of spectra. In addition, the "goodness" of fit of the factors to the experimental data was judged by how well the standard spectra of Cu foil, CuO, and Cu_2O could be modeled by the three factors.

3. RESULTS AND DISCUSSION

3.1 Commercial $CuO/ZnO/Al_2O_3$

Figure 3 illustrates the comparison of the commercial catalyst measured *in situ*, before (curve b), and during reaction (curve d) to pure standards of Cu^{2+} (curve a) and copper foil (curve c). For all of the samples, the copper edge was defined as the first inflection point of the copper metal spectrum. An examination of Fig. 3 reveals that an edge shift for the $CuO/ZnO/Al_2O_3$ catalyst taken before reaction, determined by the initial inflection point, was in close agreement with the pure Cu^{2+} standard. The slight difference in the absorption intensity was likely due to different copper contents in the path of the X-ray beam.

The sample was then exposed to the reaction mixture containing 6.9 kPa of oxygen and the experiment was performed as described in the Experimental section. After the heating ramp was complete, the activity of the catalyst was measured at 240°C while the XANES spectra were being accumulated continuously. Curved shows a sample spectrum. The copper absorption edge of 8978.5 eV for this sample corresponds exactly to the edge of the pure copper foil standard (curve c) and agrees closely with the literature value of 8979 eV (25). The energy changes of the near-edge plateau feature at $\Delta E = 4$ eV, as well as the first maximum at $\Delta E = 15$ eV, for the copper edge of the catalyst

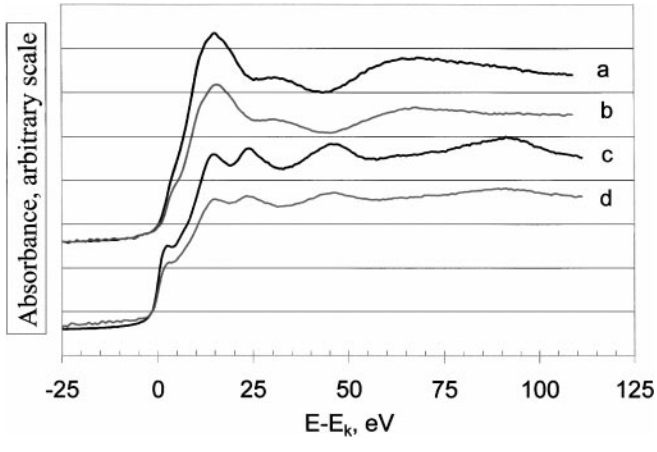

FIG. 3. XANES spectra comparing the observed absorbance of the copper-containing catalysts to those of pure phase standards: (a) cupric oxide standard; (b) $CuO/ZnO/Al_2O_3$ catalyst before reaction; (c) copper metal foil; and (d) $CuO/ZnO/Al_2O_3$ catalyst under reaction conditions at 240°C.

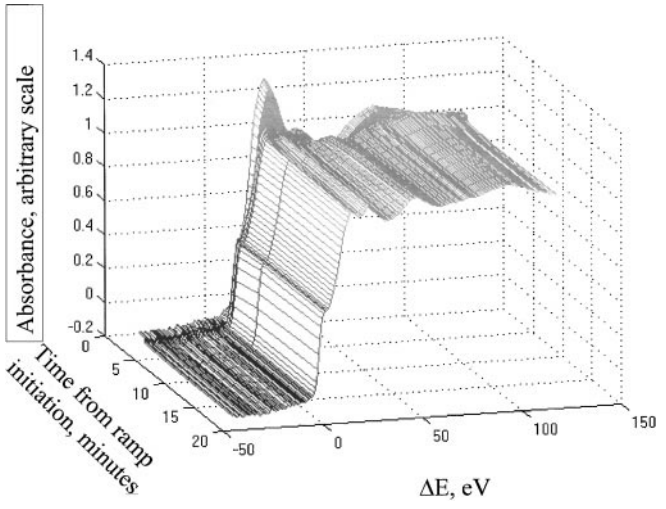

FIG. 4. Time-resolved XANES spectra of the Cu-K edge in CuO/ZnO/Al_2O_3 during the OMR reaction: $P_{O_2} = 6.9$ kPa, $P_{methanol} = 29.7$ kPa.

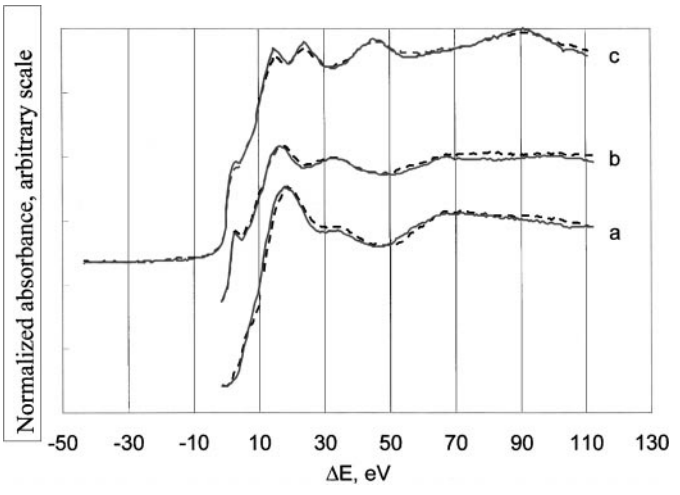

FIG. 5. Spectral comparisons of the regressed data fit using the three factors derived from data shown in Fig. 4 to the pure component standards using target testing of the factorial analysis technique. A close agreement between the spectra with the three factors and the experimental data of the standard indicates a high likelihood that a given standard is a significant component in the sample. Regressed data (- - -) and experimental data of pure component standard (—); (a) CuO, (b) Cu_2O, and (c) Cu^0.

measured at 240°C agree closely with the literature values of 2.5 and 14.9 eV, respectively (25). This indicates that the copper in the catalyst at 240°C was distinctly metallic, in stark contrast to the catalyst measured prior to the reaction run.

For each of the experiments, absorption data such as these were collected as a function of energy at an interval of 3 frames/s allowing for a rapid collection of data relative to the rate of copper reduction, which was on the order of minutes. A plot of the time-resolved XANES spectra is shown in Fig. 4. The reduction of the Cu^{2+} to metal was evidenced by examination of the disappearance of the maximum at $\Delta E = 18.7$ eV characteristic of Cu^{2+} and the appearance of the double peak edge features at $\Delta E = 16.5$ and 23.3 eV characteristic of copper metal. Additionally, the formation of the near-edge shoulder at $\Delta E = 2.5$ eV, characteristic of copper metal, also showed evidence of the reduction. The copper edge shift of −5 eV, characteristic of the reduction of CuO to copper metal, was also evident.

The change in the copper oxidation state with time was determined by evaluation of all of the copper spectra simultaneously, using the aforementioned factor analysis technique. Figures 5a–5c show the "goodness" of fit to the standards using the first three factors extracted from the experimental spectra in Fig. 4. The high degree of consistency of the components extracted from the raw data to the experimentally measured pure standards, CuO, Cu_2O, and Cu^0, conclusively indicates that the first three factors could accurately reproduce the spectra (Figs. 5a–5c). Thus, the procedure was used to analyze the data of all the experiments presented in this work.

After the factor analysis of the data in Fig. 4 was complete, the relative concentrations of the principal components (Cu^0, Cu^+, and Cu^{2+}) were obtained. These concentrations and the H_2 content in the gas phase are plotted in Fig. 6 as a function of time from the start of the temperature ramp at 180°C to 240°C for an oxygen partial pressure of 6.9 kPa. An examination of Fig. 6 and the detail in the inset showed that Cu^+ was formed as a transient phase with an observable bulk concentration up to 7 min after the start of the autothermal process. The maximum concentration of Cu^+ was 76.1% and occurred at about 4.6 min. The data suggest that the reduction of Cu^{2+} proceeded in a stepwise manner producing initially Cu^+ before the formation

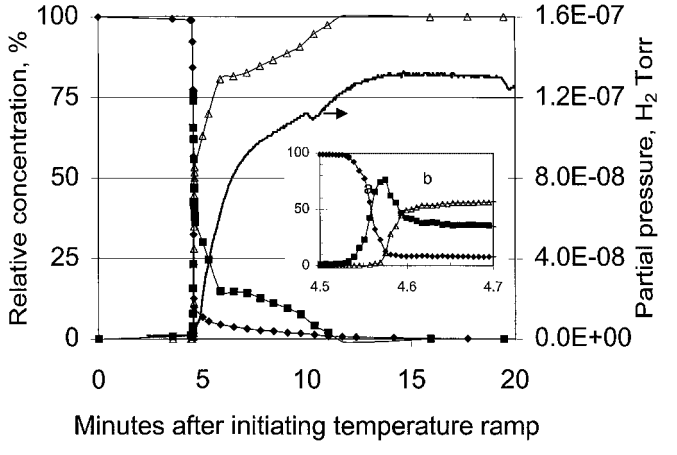

FIG. 6. Changes in the relative concentrations of different copper oxidation states in a $CuO/ZnO/Al_2O_3$ catalyst during reaction with a feed containing $P_{O_2} = 6.9$ kPa, ramp rate = 2°C/min. Inset shows magnified area from 4.5 to 4.7 min after initiation of the temperature ramp: (◆) Cu^{2+}, (□) Cu^+, and (△) Cu^0.

of metal (Eq. [7]):

$$Cu^{2+} \xrightarrow{+e^-} Cu^{+} \xrightarrow{+e^-} Cu^{0}. \qquad [7]$$

The observation of sequential reduction of Cu(II) to Cu(0) in a CuO/ZnO methanol synthesis catalysts has been reported before in a QEXAFS study (26). Our results are consistent with those reported.

Reduction of about 90% of the Cu^{2+} to lower oxidation states occurred within 3 s with a simultaneous formation of Cu^{+}. Reduction of Cu^{+} commenced when nearly all of the Cu^{2+} was gone. However, only about half of the Cu^{+} was reduced rapidly, and the remaining portion persisted for the next 5 min. H_2 production appeared to parallel the formation of Cu^{0}.

It appears as though the Cu^{+} reduction to metallic copper, shown in the inset of Fig. 6, is only slightly slower than the Cu^{2+} reduction to Cu^{+} (Fig. 6, inset (a)). This could explain the appearance of only one peak on the TPR profile for copper reduction. As in Eq. [7], if the reduction of Cu^{2+} to Cu^{+} is as facile as that of Cu^{+} to copper metal under these conditions, then it is reasonable to expect that no separation of reduction peaks would be observed under the more reducing conditions used for TPR.

3.2. Effect on the OMR Reaction of Oxygen Partial Pressure

The dependence of the reduction of CuO on the oxygen partial pressure was examined at two other oxygen pressures, $P_{O_2} = 3.4$ kPa and 12.7 kPa, which corresponded to oxygen/methanol molar ratios of 0.10 and 0.41, respectively. These studies were in addition to the data in Fig. 6 for a P_{O_2} of 6.9 kPa and an oxygen/methanol ratio of 0.23. If the only reaction products of methanol were H_2, CO_2, and H_2O, the enthalpy of reaction at complete conversion for the previously mentioned oxygen partial pressures would be 73.7, −103.6, and −0.7 kJ/mol, respectively, and the H_2 concentration in the effluent would be 73.7%, 59.4%, and 69.2%, respectively.

Increasing the oxygen partial pressure from 6.9 kPa to 12.7 kPa resulted in a substantial increase in the rate of Cu^{2+} reduction in the area of the beam-path as shown in Fig. 7. Similar to the results in Fig. 6, a transient formation of Cu^{+} was detected. Within 2 s of the autothermal transition initiation all of the Cu^{2+} is consumed with nearly complete formation of copper metal. Decreasing the oxygen partial pressure to 3.4 kPa resulted in a decrease in the reduction rate of Cu^{2+}, as shown in Fig. 8. Cu^{+} was readily detectable for a 13-min interval with a maximum concentration of 44%, while metallic copper formation lagged the Cu^{+} by about 5 min. The initial reduction of the catalyst was relatively rapid with the Cu^{2+} content dropping from 96% to 87% in less than 40 s. It has been shown previously that the available Cu^{2+} on the commercial $CuO/ZnO/Al_2O_3$ catalyst is about 11 ± 3.5 m^2/g or 4%

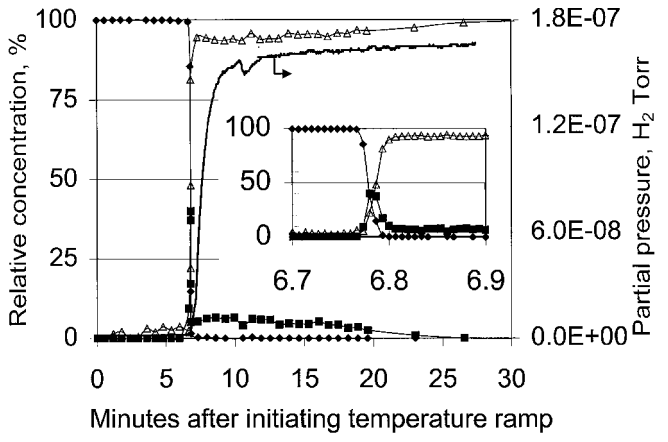

FIG. 7. Changes in the relative concentration of different copper oxidation states in a $CuO/ZnO/Al_2O_3$ catalyst during reaction with a feed containing $P_{O_2} = 12.9$ kPa, ramp rate = 2°C/min. Inset shows magnified area from 6.7 to 6.9 min after initiation of the temperature ramp: (◆) Cu^{2+}, (□) Cu^{+}, and (△) Cu^{0}.

dispersion (15). Within experimental uncertainty, it is possible that this rapid reduction is indicative of the immediately accessible copper surface. The increase in reduction rate due to increasing oxygen partial pressure is an interesting observation. It is likely a result of the exothermicity of the methanol oxidation reaction (Eq. [3]). As shown previously in the presence of even a low oxygen concentration, methanol undergoes oxidation almost exclusively with very little steam reforming occurring (15). The rate of the oxidation reaction increases with oxygen partial pressure, resulting in an increase in heat generation. Thus, the catalyst wafer was heated more rapidly, resulting in a faster consumption of oxygen upstream from the beam and a more rapid rate of reduction of the copper in the region where no available gas phase oxygen was present near the wafer.

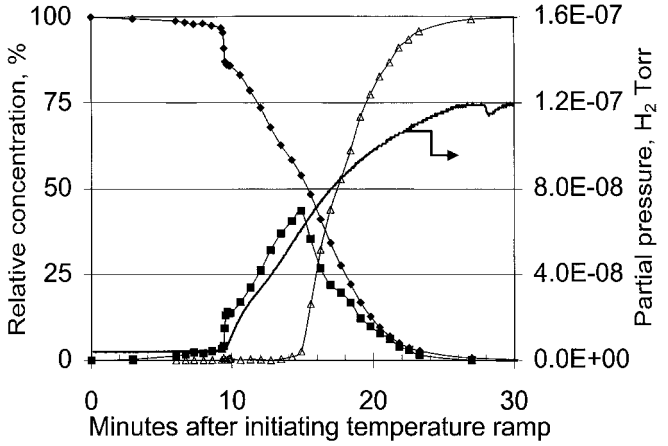

FIG. 8. Changes in the relative concentration of different copper oxidation states in a $CuO/ZnO/Al_2O_3$ catalyst during reaction with a feed containing $P_{O_2} = 3.4$ kPa, ramp rate = 2°C/min; (◆) Cu^{2+}, (□) Cu^{+}, and (△) Cu^{0}.

The data for all three partial pressures of oxygen show that a portion of the copper was reduced much faster than the remaining copper. This is likely because the rate of reduction of the core of a particle of copper oxide is limited by the relatively slow diffusion of oxygen ions through the lattice. The diffusion limitation apparent in these runs can be observed by examination of TPR evidence of two pure CuO samples varying only by surface area. The reduction of a pure CuO sample with a surface area of <1 m^2/g occurred with a maximum H_2 consumption rate at 300°C, which was 50°C higher than that of a sample having a surface area of 20 m^2/g, suggesting that diffusion of oxygen is the rate-limiting phenomenon in the reduction of copper catalysts.

The H_2 concentration in the effluent stream paralleled the formation of metallic copper in Figs. 6 and 7, suggesting that metallic copper is the active phase for methanol steam reforming. However, for the data in Fig. 8 for $P_{O_2} = 3.4$ kPa, H_2 appeared to be produced before metallic copper was detected. It is suspected that it is an artifact as a consequence of the measurement. The X-ray beam probed only a small portion of the catalyst wafer. It is possible that in this experiment, the beam was probing the portion nearer the entrance of the feed gas mixture. Because of the low partial pressure of O_2, by the time Cu^+ began to be detected in the beginning portion of the catalyst wafer, oxygen was consumed completely in the latter portion of the catalyst wafer, where the copper was already reduced to metallic copper active for H_2 production. Additional results described in the next section supported this interpretation. It should be noted that since the thickness of the catalyst wafer was only a fraction of the cross-sectional area of the sample chamber, some of the reactant stream would pass through without contacting the wafer. Therefore, it was not possible to make meaningful comparisons of the product distribution from this apparatus with those of a conventional packed-bed reactor. Furthermore, oxygen could be entirely consumed in the gas mixture near the sample wafer even when it was still detectable at the exit of the sample chamber.

3.3. Reoxidation of the Reduced Catalyst

Reoxidation of the catalyst was examined by following the copper oxidation states as the reactor was cooled from 240°C to 100°C for the experiments using P_{O_2} of 3.4 kPa (Fig. 9). There was no detectable reoxidation of metallic copper until the temperature of the catalyst reached about 170°C (5.4 min after commencement of cooling), when Cu^+ appeared. Reoxidation to Cu^+ was mostly complete within 5 min after it began, but there was no further oxidation to Cu^{2+}. The H_2 concentration in the effluent seemed to be related to the copper concentration profile. When metallic copper was the principal phase, the partial pressure of H_2 decreased due to the decreasing temperature in the reactor during cooling. However, after 5.4 min when the formation of Cu^+ became significant, a substantial decrease in

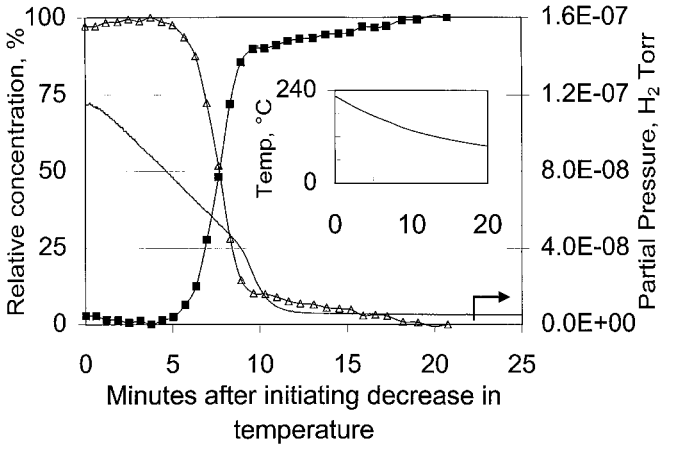

FIG. 9. Changes in the relative concentrations of different copper oxidation states in a $CuO/ZnO/Al_2O_3$ catalyst during cooling of the reactor from 240°C: $P_{O_2} = 3.4$ kPa; (□) Cu^+ and (△) Cu^0. Inset shows the temperature measured by the thermocouple inserted in the reactor.

H_2 was evident, suggesting deactivation of the active copper metal by reoxidation. Thus, H_2 production appeared to be associated with metallic copper only. The absence of Cu^{2+} formation is likely due to the slow diffusion of lattice oxygen at these low temperatures.

3.4. Characterization of Samples after a Reduction–Oxidation Cycle

In addition to the previously described experiments, multiple cycles of oxidation and reduction were studied to determine longer-term performance. A 23% CuO/ZnO was chosen as the test system. XRD data of the sample showed that the CuO particle size of the 23% CuO/ZnO sample, estimated by the Scherrer equation, was approximately double that of a fresh commercial catalyst. The catalyst was pressed into a wafer, placed into the *in situ* cell, and the experiment proceeded as shown previously with an oxygen partial pressure of 6.9 kPa. During the initial ramp, the CuO/ZnO catalyst, shown in Fig. 10, was reduced much more rapidly than the commercial catalyst illustrated in Fig. 6 for the same P_{O_2}. As with the commercial samples, Cu^+ appears as a transient species suggesting that Cu^{2+} was reduced first to Cu^+ before the appearance of metallic copper. After the ramp was complete and the copper was observed to be completely reduced, steady state conversions were determined at 240°C.

Once the activity measurements were finished, the temperature was lowered from 240°C to 100°C, the reactor was allowed to cool, and the copper oxidation states were again monitored. During the temperature decrease, the catalyst remained completely reduced during the majority of the experiment (Fig. 11). As in previous runs, the H_2 partial pressure was also observed to decrease in a steady fashion, presumably due to the reforming rate dependence with

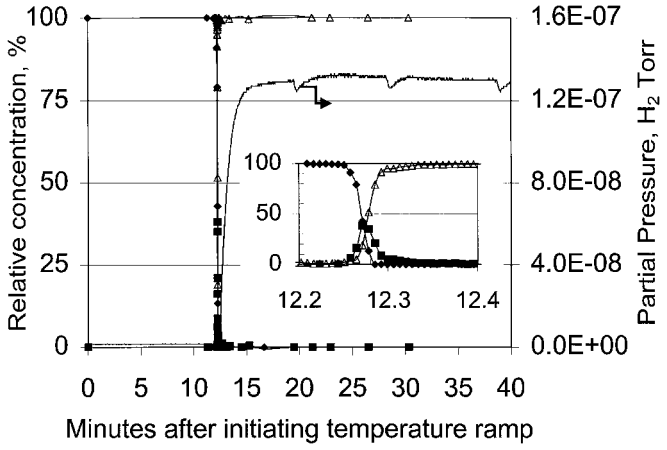

FIG. 10. Changes in the relative concentrations of different copper oxidation states in a 23% CuO/ZnO catalyst during reaction with a feed containing $P_{O_2} = 6.9$ kPa, ramp rate = 2°C/min; (◆) Cu^{2+}, (□) Cu^{+}, and (△) Cu^{0}.

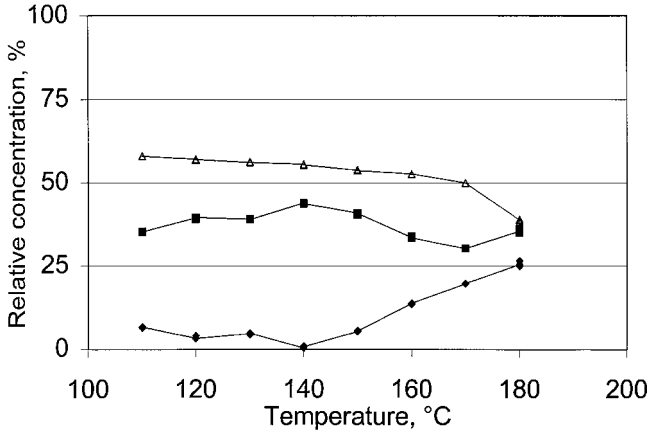

FIG. 12. Copper oxidation state spot check as a function of temperature during catalyst recycle for 23% CuO/ZnO: $P_{O_2} = 6.9$ kPa, ramp rate = 5°C/min; (◆) Cu^{2+}, (□) Cu^{+}, and (△) Cu^{0}.

temperature. However, in this case no reoxidation of the catalyst was observed during the steady decrease in the reforming rate. At 14 min after cool-down initiation, the reactor temperature leveled off at 150°C for a few seconds and then dropped off dramatically. This was followed by a rapid reoxidation of the copper metal to Cu^{+} and a commensurate decline in H_2 partial pressure. Interestingly, there was not a complete reoxidation of copper metal to Cu(I) that was observed with the commercial sample. This may be due to the larger copper particle size in this sample, such that the Cu^{0} in the core is slower to be reoxidized.

After the sample reached 100°C, a second heating cycle was initiated, and the temperature was steadily increased to 180°C. During this ramp up to measure oxidizing activity, XANES spot checks were determined every 10° until 180°C and are shown in Fig. 12. Minimal reoxidation of the bulk copper was observed until approximately 140°C. At that point, Cu^{2+} began to appear signaling the initiation of oxidizing activity. Steady reoxidation with temperature was observed until at 180°C, Cu^{2+}, Cu^{+}, and metallic copper were 30%, 50%, and 20%, respectively. At this point the oxidation activity of the catalyst was measured. Catalyst activity and product selectivity were found to be essentially identical to those of a fresh sample. After the oxidation activity was determined, the ramp was initiated and XANES data were acquired again until 240°C (Fig. 13). Only minimal additional reoxidation of the bulk copper was observed before the reduction of the copper, which occurred 10.7 min after ramp initiation, suggesting that reoxidation of the bulk was slow. However, the recovery of the catalytic oxidation activity suggests that the surface of the copper catalyst was completely oxidized to Cu^{2+}.

The catalyst appeared to behave similarly for the first and second reduction cycles. Only a minor decrease in the activation temperature from 240°C to 201°C was observed

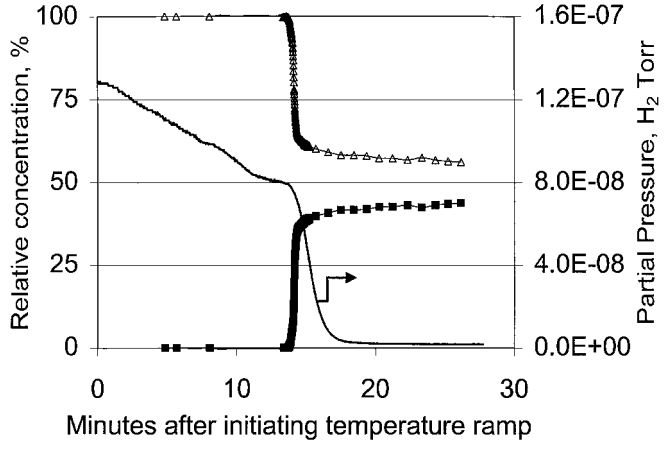

FIG. 11. Changes in the relative concentrations of different copper oxidation states in a 23% CuO/ZnO catalyst during cooling of the reactor from 240°C. $P_{O_2} = 6.9$ kPa; (□) Cu^{+}, and (△) Cu^{0}.

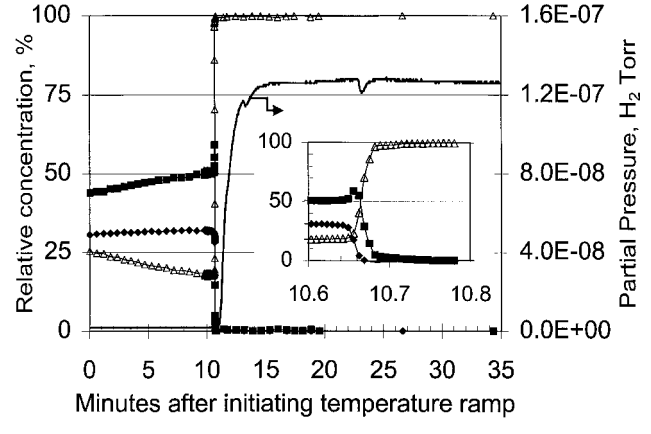

FIG. 13. Changes in the relative concentrations of different copper oxidation states in a 23% CuO/ZnO catalyst during the second cycle reaction with a feed containing $P_{O_2} = 6.9$ kPa, ramp rate = 2°C/min; (◆) Cu^{2+}, (□) Cu^{+}, and (△) Cu^{0}.

with the second cycle. The time for complete removal of the Cu^{2+} phase is shorter in the second reduction cycle. This is likely due to the relatively small amount of CuO present in the second cycle. All of the copper is predominantly metallic copper within 2 s after reduction commencement for both the first and second reduction cycles.

4. CONCLUSIONS

A copper-containing catalyst has been shown to perform more than one function in the oxidative methanol reforming reaction. For small oxygen conversions, oxidation is predominant over the Cu^{2+} phase with only minimal selectivity to H_2. As the oxygen conversion nears completion, the copper is rapidly reduced to metal. Reforming activity with principal selectivity to H_2 is observed over a reduced catalyst. The *in situ* XANES measurements showed clearly that Cu^0 is needed for steam reforming.

Increasing oxygen partial pressure resulted in more rapid reduction of a majority of the catalyst because of more severe local heating of the catalyst by the faster combustion of methanol and depletion of oxygen. For all of the samples, the reduction of Cu^{2+} to Cu^0 proceeds via Cu^+ which has not been associated with significant activity for either oxidation or reforming.

A number of limitations imposed by the apparatus mentioned earlier prevented quantitative treatment of the data presented here. These include not knowing the exact temperature of the sample wafer, nonuniform temperature distribution across the wafer, the X-ray beam probing only a small portion of the wafer, bypassing of the reactants, and the long lag time in detection of the products compared with the rate of changes in the sample. However, meaningful and useful conclusions can still be drawn from qualitative comparisons especially when the entire set of data is considered together.

Many of the issues surrounding long-term performance of an operational $CuO/ZnO/Al_2O_3$ catalyst remain unresolved. However, much is now known about the initial performance of the catalyst as well as its activation process. Such information should be useful in developing strategies that allow a more fundamental approach to eliminate the remaining obstacles to implementation of these systems for automotive use.

ACKNOWLEDGMENTS

The work at the Advanced Photon Source was supported by the U.S. Department of Energy under Contract No. W-31-109-ENG-38. Discussions on principal component analysis with S. Wasserman and assistance with the experimental setup by A. Mashayekhi and T. Middleton and financial support by Argonne National Laboratory are gratefully acknowledged.

REFERENCES

1. Meitzner, G., and Iglesia E., *Catal. Today* **53**, 433 (1999).
2. Clausen, B. S. Gråbaek, L., Steffensen, G., Hansen, P. L., and Topsøe, H., *Catal. Lett.* **20**, 23 (1993).
3. Clausen, B. S., and Topsøe, H., *Catal. Today* **9**, 189 (1991).
4. Rodriguez, J. A., Hannson, J. C., Chatuvedi, S., Maiti, A., and Brito, J. L., *J. Chem. Phys.* **112**, 935 (2000).
5. Coulston, G. W., Bare, S. R., Kung, H. H., Birkeland, K., Bethke, G., Harlow, R., and Lee, P. L., *Science* **275**, 191 (1997).
6. Jiang, C. J., Trimm, D. L., Wainwright, M. S., and Cant, N. W., *Appl. Catal.* **93**, 245 (1993).
7. Jiang, C. J., Trimm, D. L., Wainwright, M. S., and Cant, N. W., *Appl. Catal.* **97**, 145 (1993).
8. Takezawa, N., and Iwasa, N., *Catal. Today* **36**, 45 (1997).
9. Peppley, B. A., Amphlett, J. C., Kearns, L. M., and Mann, R. F., *Appl. Catal. A* **179**, 21 (1999).
10. Peppley, B. A., Amphlett, J. C., Kearns, L. M., and Mann, R. F., *Appl. Catal. A* **179**, 31 (1999).
11. Kumar, R., Ahmed, S., Krumpelt, M., and Myles, K. M., Argonne National Laboratory Report, ANL-92/31. Argonne National Laboratory, Argonne, IL, 1992.
12. Kumar, R., Ahmed, S., and Krumpelt, M., 1996 Fuel Cell Seminar Program and Abstracts, p. 750, 1996.
13. Breen, J. P., and Ross, J. R. H., *Catal. Today* **51**, 521 (1996).
14. Reitz, T. L., Ahmed, S., Krumpelt, M., Kumar, R., and Kung, H. H., Proc. 12th Intern. Cong. Catal. *Stud. Surf. Sci. Catal.* **130**, 3645 2000.
15. Reitz, T. L., Ahmed, S., Krumpelt, M., Kumar, R., and Kung, H. H., *J. Mol. Catal. A: Chemical* **162**, 275 (2000).
16. Lee, P. L., Beno, M. A., Jennings, G., Ramanathan, M., Knapp, G. S., Huang, K., Bai, J., and Montano, P. A., *Rev. Sci. Instrum.* **1**, 65 (1994).
17. Brauer, S., Rodricks, B., Assoufid, L., Beno, M. A., and Knapp, G. S., *Rev. Sci. Instrum.* **9**, 67 (1996).
18. Phizackerley, R. P., Rek, Z. U., Stephenson, G. B., Conradson, S. D., Hodgson, K. O., Matsushita, T., and Oyanagi, H., *J. Appl. Crystallogr.* **16**, 220 (1983).
19. Malet, P., and Caballero, A., *J. Chem Soc., Faraday Trans.* **84**, 2369 (1988).
20. Fierro, G., Lo Jacono, M., Inversi, M., Porta, P., Lavecchia, R., and Cioci, F., *J. Catal.* **148**, 709 (1994).
21. Fierro, G., Lo Jacono, M., Inversi, M., Porta, P., Cioci, F., and Lavecchia, R., *Appl. Catal. A* **137**, 327 (1996).
22. Monti, D. A. M., and Baiker, A., *J. Catal.* **83**, 353 (1983).
23. Malinowski, E. R., and Howery, D. G., "Factor Analysis in Chemistry." Wiley, New York, 1980.
24. Wassermann, S. R., Allen, P. G., Shuh, D. K., Bucher, J. J., and Edelstein, N. M., *J. Synchrotron Rad.* **6**, 284 (1999).
25. Bearden, J. A., and Burr, A. F., *Rev. Mod. Phys.* **39**, 125 (1967).
26. Als-Nielsen, J., Grübel, G., and Clausen, B. S., *Nucl. Instrum. Methods Phys. Res. B* **97**, 522 (1995).